

A Cylindrical Structure of the 200-pc Molecular Ring in the Galactic Center

YOSHIAKI SOFUE *Institute of Astronomy, University of Tokyo, Mitaka, Tokyo 181, Japan*

(Received July 24, 1989; in final form September 12, 1989)

The 200-pc expanding ring in the Galactic center is shown to have a cylindrical shape extending in the direction perpendicular to the galactic plane with the vertical extent of more than 150 pc. The association of the radio continuum emission indicates that the cylinder is a mixture of molecular and ionized hydrogen gases. We also suggest that the extended high-temperature plasma recently detected in the galactic center may compose an interior hot component of the cylinder. We discuss the formation mechanism of the cylindrical structure based on an explosion/starburst model.

KEYWORDS Activity Galactic Expanding ring Galactic center Molecular gas
Radio emission The Galaxy X-rays.

1. INTRODUCTION

The 200-pc expanding ring of molecular gas found in the galactic center (Kaifu *et al.*, 1972, 1974; Scoville, 1972) has long been studied as a particular object in our Milky Way. However, it has been supposed that a similar ring feature may exist in external galaxies with an activity in the center. Recent high-resolution molecular-line observations of external galaxies have revealed that galactic nuclei are often associated with similar expanding rings (e.g. Nakai *et al.*, 1987). It is now believed that an expanding ring is not a particular phenomenon found in our Galaxy, but a rather common feature as the manifestation of an explosive energy release at the nucleus.

Various models have been proposed for the formation mechanism of the expanding ring in the nuclear region based mainly on the assumption that the rings are produced by shock waves driven by an intense energy release at the nuclei (Saito and Saito, 1977; Sofue, 1976, 1977, 1984; Tomisaka and Ikeuchi, 1987; Umemura *et al.*, 1987). Most of the models have shown that an explosive energy release such as due to a single explosion or a series of supernova explosions in a starburst results in the formation of an expanding cylinder extending perpendicular to the galactic plane rather than a torus confined in the disk.

It is therefore likely that the 200-pc molecular ring in our Galaxy may have an elongated structure forming a cylinder extending perpendicular to the galactic plane. It is also probable that such an energetic shock may be associated with ionized thermal gas as well as a very high-temperature component emitting X-rays, which are indeed found to be associated with a molecular cylinder in the starburst galaxy M82 [see, e.g., Nakai *et al.*, (1987)].

In the present paper we revisit this prominent ring feature in the galactic center in order to clarify if it is really a similar structure to that often observed in external galactic nuclei (see, e.g., Nakai *et al.*, 1987). We point out a cylindrical structure of the molecular ring, and discuss the formation mechanism in relation to the activity in the center of the Galaxy. For this purpose we not only examine the molecular line emission but also investigate radio continuum features associated with the 200-pc ring as well as the IRAS far-infrared data. In particular, modern survey data both in the radio continuum (Reich *et al.*, 1984; Handa *et al.*, 1987) and CO lines (Bally *et al.*, 1987, 1988) with comparable angular resolutions give the opportunity to study a spatial relationship between the molecular and HII gases and/or nonthermal emission in the galactic center region. Finally we suggest that the recently detected hot (10 keV) plasma near the galactic center (Koyama *et al.*, 1989) may possibly be related to the expanding cylinder, composing its interior hot component.

2. CYLINDRICAL STRUCTURE OF THE 200-PC MOLECULAR RING

2.1. Radio and CO Maps

The ^{13}CO ($J=1-0$) line survey by Bally *et al.*, (1987) covers a region of $-5^\circ < l < 5^\circ$, $-0^\circ.6 < b < +0^\circ.6$ at an angular resolution of $6'$ ($=[(\text{HPBW})^2 + (\text{grid spacing})^2]^{1/2}$). The continuum survey data at 10 GHz (Handa *et al.*, 1987) have a resolution of $2'.7$, and the 2.7 GHz data (Reich *et al.*, 1984) have a resolution of $4'.3$. The fact that their angular resolutions are comparable to each other provides a good opportunity to make a comparative study among them.

In order to carry out this comparison, however, we must be careful about the fact that the molecular line emission is dominated by the emission from dense clouds in the central few hundred parsecs, and their scale sizes are typically less than a few tens of arc minutes, or smaller than ~ 100 pc. On the other hand the continuum emission is significantly contaminated by the diffuse galactic disk emission, which is the sum of emissions along the line sight for an 8 kpc path length, and include larger-scale emission structures.

For this reason we first smooth the radio continuum maps by a convolution with a Gaussian function of a $6'$ HPBW. It is also better to subtract the diffuse emission from the continuum maps, and compare only the small-scale continuum structures with the molecular gases. For this we apply a background-filtering technique (BGF; Sofue and Reich, 1979) to the continuum maps with filtering beam sizes of $0^\circ.4$, $0^\circ.2$ and $0^\circ.1$. Here the filtering sizes were chosen for the reason that structures in the central few hundred parsecs may typically have scale sizes comparable to or smaller than the scale thickness of the nuclear disk.

In Figure 1 we compare the various maps in the same scale. Figure 1a is a $V_{\text{LSR}} - l$ diagram of the CO line emission, and Figure 1b shows the CO intensities integrated within $-100 < V_{\text{LSR}} < -20 \text{ km s}^{-1}$ for $l < 0^\circ$ and $20 < V_{\text{LSR}} < 100 \text{ km s}^{-1}$ for $l > 0^\circ$, respectively [reproduced from Bally *et al.* (1987, 1988)]. In Figure 1c we show the BGF continuum map with the filtering beam of $0^\circ.4$ and smoothed to a $6'$ angular resolution made from the 2.7 GHz survey (Reich *et al.*, 1984). Figure

1d is the same but made from the 10 GHz survey (Handa *et al.*, 1987). In Figure 1e we show the far-infrared emission at $60\ \mu\text{m}$ of the same area made from the IRAS data (Beichman *et al.*, 1985) also obtained by applying the BGF method and smoothing to the same angular resolution.

2.2. The 200-pc Expanding Ring and its Vertical Extension

The 200-pc expanding molecular ring is seen as a tilted ellipse in the $V_{\text{LSR}} - l$ (velocity-longitude) diagram (Figure 1a). The ellipse can be fitted by a superposition of an expansion at a velocity of $110\ \text{km s}^{-1}$ and a rotation at $70\ \text{km s}^{-1}$.

On the distribution maps of the CO intensity integrated for the range $+20 \leq V_{\text{LSR}} \leq +100\ \text{km s}^{-1}$ and for $-100 \leq V_{\text{LSR}} \leq -20\ \text{km s}^{-1}$, the tangential cross sections of the ring appear as enhancements at $l = 1^\circ.4$ and $-1^\circ.2$ (Figure 1b). The angular diameter of the ring is therefore $2^\circ.6$ and the linear radius is $r \approx 180\ \text{pc}$ for a distance of 8 kpc.

It is remarkable that the cross sections are associated with spurs that extend in the direction perpendicular to the galactic plane. The spur ridge at $l = 1^\circ.4$ is slightly shifted toward the positive latitude side and can be traced from $b \sim -0^\circ.4$ to $+0^\circ.5$. The spur at $l = -1^\circ.2$ can be traced only below the galactic plane and extends at least up to $b = -0^\circ.6$.

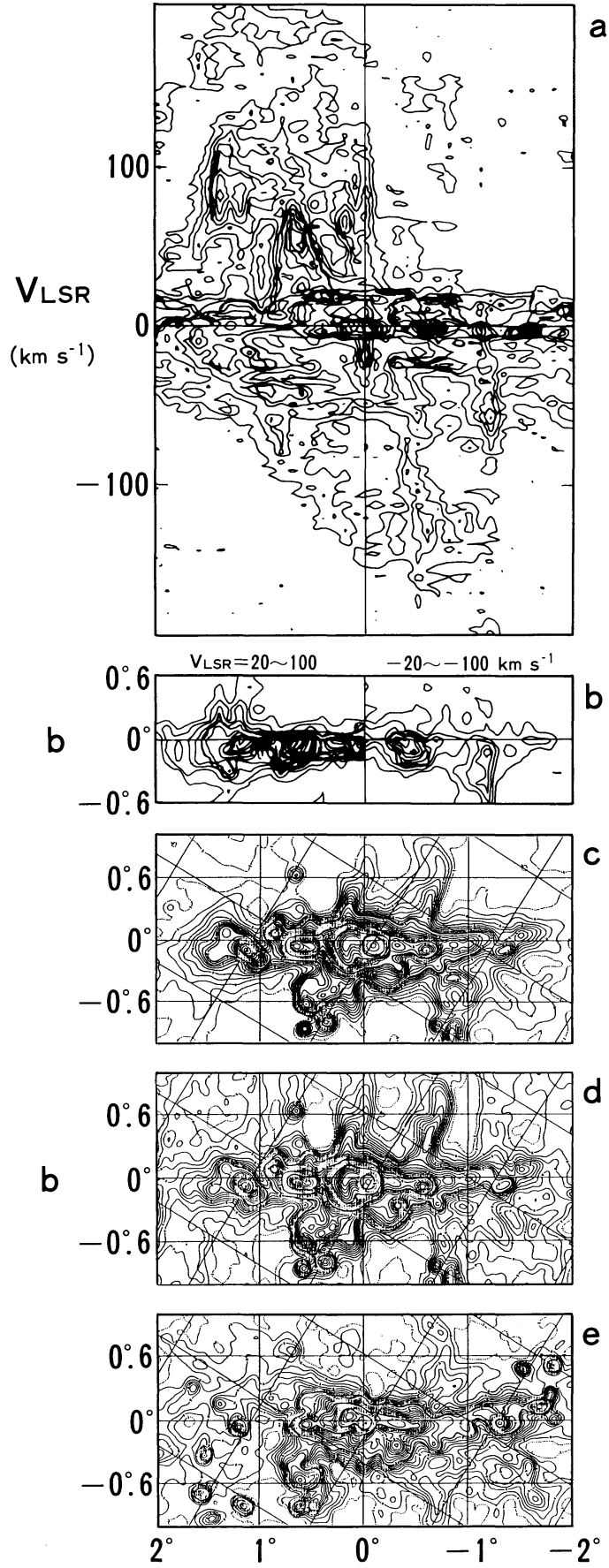
At a distance of 8 kpc the vertical length of the spur seen in the present CO maps is about 150 pc on the positive longitude side and 90 pc on the negative longitude side. Since the observations do not cover higher-latitude region, these lengths may be lower limits, and the spur may extend farther. By contrast, the thickness of the spur ridge is as thin as $\sim 0^\circ.1$, or 15 pc, an order of magnitude smaller than the vertical and radial extents.

This fact indicates that the expanding molecular ring is not a structure confined within the galactic disk, but extends toward the region high above the galactic plane. In fact, the mean thickness of the CO disk determined from the CO gas distribution in Figure 1b is some 40 pc ($0^\circ.3$). The vertical extension may indicate that the 200-pc (180-pc) ring has a cylindrical shape with its wall perpendicular to the disk plane, and a vertical extent of more than 150 pc, several times the nuclear-disk thickness.

2.3. Radio continuum spurs and far-IR emission associated with the 200-pc ring

Radio continuum maps in the central few hundred parsecs reveal a number of spurs which emerge from the galactic plane. Near the tangential direction of the 200-pc ring at $l = 1^\circ.4$, we can recognize enhancements in the continuum emission. If we apply the background-filtering technique to the map at 2.7 GHz (Figure 1c), an arc-like spur is enhanced. The spur extends from the galactic plane at $l = 1^\circ.4$ to $l = 1^\circ.2$, $b = 0^\circ.4$, and follow the extent of the CO spur. From a comparison with a 10-GHz map (Figure 1d) the radio spectral index toward the spur is flat, which suggests its thermal origin. Association of a radio spur at negative longitude is not clear because of the disturbance by the nearby strong nonthermal radio source, G359.1-0.9, a shell-type supernova remnant.

In Figure 1e we show a BGF map of the $60\ \mu\text{m}$ emission for the same region,



where the background structures with scale sizes greater than $0''.4$ are again subtracted. The spurs are identified on the FIR (far-infrared) emission map of IRAS at $60\ \mu\text{m}$ (Beichman *et al.* 1985). It is known that radio continuum features associated with the FIR emission are mostly thermal objects (HII regions), while those not associated with FIR emission are of nonthermal origin like supernova remnants (Fürst *et al.*, 1987; Reich *et al.*, 1987). More precisely, the ratio of $60\text{-}\mu\text{m}$ intensity to radio-continuum intensity at 2.7 GHz for thermal objects like HII regions is between 1000 and 2000 and vice versa, while if the ratio is less than ~ 300 , the radio emission is non-thermal. Using the IRAS and radio continuum maps we obtain the result that the FIR($60\ \mu\text{m}$)-to-radio (2.7 GHz) intensity ratio is approximately ~ 1500 toward the continuum spur at $l \approx 1^\circ.4$, $b \approx 0^\circ.3$. This fact indicates that the spur is a thermal object, consistent with the flat radio spectrum. [See Reich *et al.* (1987) for a discussion of the thermal and nonthermal emission structures in the central region.]

2.4. Hot plasma

We briefly discuss here a possible relation of the 200-pc expanding cylinder with the recently detected hot plasma that may be a shock-heated gas at a temperature of 10 keV ($\sim 10^8$ K) (Koyama *et al.* 1989). The plasma was detected via its iron X-ray line radiation at 6.7 keV with the Ginga Satellite. The emission region is extended with a size of $1^\circ.8$ (250 pc) about the galactic center. We should emphasize that the observed size of the plasma region is approximately the same as the extent (360 pc diameter) of the 200-pc (180-pc) molecular cylinder. Considering the angular resolution of the detector and data-sampling grids, we may conclude that the plasma is situated surrounded by the cylinder.

It is therefore likely that the plasma consists of an interior hot component which is a remnant of shock-heated gas from an explosive event at the nucleus when the expanding motion had a velocity of $>10^3\ \text{km s}^{-1}$. Since the cooling time of this plasma, 4×10^8 yr, is fairly long compared to the time scale of the expanding cylinder, several 10^6 yr (=radius/expansion velocity), it is possible that the hot component remains uncooled, being walled-in by the 200-pc molecular cylinder. We note that, unless the plasma appeared only very recently, say within 10^5 yr, it is impossible to confine such a high-temperature gas within a volume of some 250-pc size, because the sound velocity, and therefore its free-expansion, is as high as $10^3\ \text{km s}^{-1}$.

FIGURE 1 Comparison in the same scale of $^{13}\text{CO}(J=1-0)$ data with the radio continuum emission maps: (a) The $V_{\text{LSR}}-l$ diagram of the CO gas (taken from Bally *et al.*, 1987). (b) CO intensity distributions integrated in the velocity ranges from 20 to $100\ \text{km s}^{-1}$ for $l \geq 0^\circ$, and from -20 to $200\ \text{km s}^{-1}$ for $l \leq 0^\circ$ (taken from Bally *et al.* 1987). (c) A BGF (background-filtered) radio continuum map at 2.7 GHz (Reich *et al.*, 1984) with the background emission with scale sizes greater than $0''.4$ being subtracted and smoothed to $6'$ resolution. The hatched contours are at 0.3, 1, 3 and $10\ \text{K } T_{\text{B}}$. (d) A BGF radio continuum map at 10 GHz (Handa *et al.*, 1987) with the background emission of scale sizes greater than $0''.4$ being subtracted and smoothed with a Gaussian function of $6'$. The lowest dashed contours are at 0 K. Thick (hatched) contours are at 3, 10, 30 and $100\ \text{K } T_{\text{B}}$. (e) A BGF far-infrared map at $60\ \mu\text{m}$ made from the IRAS data with the background emission of scale sizes greater than $0''.4$ being subtracted and smoothed to $6'$ resolution. The hatched contours are at 3, 10, 30 and $100\ \text{Jy/beam}$.

2.5. Masses and Energetics

(a) Molecular gas. The column density of hydrogen molecules is given by $N(\text{H}_2) \sim 2 \times 10^{21} I \text{ cm}^{-2}$, or the surface mass density is $\sigma \sim 32 I M_\odot \text{ pc}^{-2}$, where $I \equiv \int T_A^* dv$ (in K km s^{-1}) is the integrated intensity of ^{13}CO emission (Solomon *et al.* 1979). Since the observed ^{13}CO intensity toward the 200-pc ring is roughly $\sim 50 \text{ K km s}^{-1}$ (Bally *et al.* 1988) and the line-of-sight depth of the ring is about 100 pc, we obtain a mean molecular hydrogen density of the order of $\sim 300 \text{ H}_2 \text{ cm}^{-3}$ toward $l \sim 1^\circ.2$.

Using the $(V_{\text{LSR}} - l)$ diagram averaged in the range $-0^\circ.6 \leq b \leq +0^\circ.6$ (Bally *et al.*, 1988), we integrated the intensity of the 200-pc ring (cylinder) and obtained the total H_2 mass,

$$M \sim 32 \int \int \int T_A^* dv dx dy [M_\odot] \sim 2.3 \times 10^7 M_\odot,$$

where x and y (in pc) are linear distances in the l and b directions, respectively. Since the expansion velocity is about 110 km s^{-1} , this leads to a total kinetic energy of expansion of $\sim 3 \times 10^{54}$ ergs.

Kaifu *et al.* (1972) and Scoville (1972) gave a mass and an expansion energy of the ring of $10^8 \sim 10^9 M_\odot$ and $10^{55} \sim 10^{56}$ ergs, respectively, while Kaifu *et al.* (1974) gave a smaller value, $\sim 4 \times 10^{54}$ ergs. The present estimate gives smaller values by almost an order of magnitude compared to the former values, even if we take into account the larger distance to the galactic center (10 kpc) adopted at that time, while it agrees with the more recent value obtained by Kaifu *et al.* (1974). The difference may be a result from the fact that the estimates by Kaifu *et al.* (1972) and Scoville (1972) were based on an assumption of a uniform density of $10^{3-4} \text{ H}_2 \text{ cm}^{-3}$ in the ring, while the present estimate is the result of a direct integration of the ^{13}CO data.

However, since it is reasonable to assume that CO emission comes from regions of H_2 density of the order of 10^{3-4} cm^{-3} , the lower total mass obtained here may indicate that the 200-pc ring is not a structure of uniform density but rather has a clumpy structure composed of molecular clouds and/or filaments with a filling factor of about ~ 0.1 . Such a clumpy structure is in fact seen from the $V_{\text{LSR}} - l$ diagram of ^{13}CO emission (Bally *et al.* 1987, 1988).

(b) HII gas in the cylinder. The observed brightness of the thermal radio emission is about 100 mK toward the spur associated with the 200-pc cylinder. If we assume an optically thin ionized gas of $T_e \sim 10^4 \text{ K}$ and $T_B \sim 0.1 \text{ K}$ at $\nu = 10 \text{ GHz}$, we obtain an emission measure of $EM \sim 4000 \text{ pc cm}^{-6}$. We then obtain a thermal electron density $n_e \sim 6 \text{ cm}^{-3}$, and the total mass of HII gas is derived to be $\sim 4 \times 10^5 M_\odot$ for the same geometry as the molecular cylinder (radius 180 pc, width 15 pc, and vertical extent 150 pc). Then the thermal energy involved in the cylinder is of the order of $\sim 10^{51}$ ergs.

(c) Hot interior. The total X-ray luminosity from the extended 10-keV plasma is estimated to be $L_X \sim 3 \times 10^{37} \text{ erg s}^{-1}$ for a distance of 8 kpc (Koyama *et al.*, 1989). Assuming a thin thermal plasma with a temperature of $1.2 \times 10^8 \text{ K}$

TABLE I
Derived parameters for the 200-pc expanding cylinder*

[The 200-pc cylinder]	
Ring (cylinder) radius	180 (± 5) pc
Rotation velocity	70 (± 10) km s ⁻¹
Expansion velocity	110 (± 5) km s ⁻¹
Vertical extent of the cylinder	~ 150 pc
Thickness of the cylinder	~ 15 pc
H ₂ mass	$\sim 2.3 \times 10^7 M_{\odot}$
HII mass	$\sim 4 \times 10^5 M_{\odot}$
Kinetic energy of expanding motion	$\sim 3 \times 10^{54}$ ergs
Thermal energy	$\sim 10^{51}$ ergs
[Interior hot gas]	
X-ray luminosity†	$\sim 3 \times 10^{37}$ ergs s ⁻¹
Mass of hot plasma	$\sim 2 \times 10^4 M_{\odot}$
Thermal energy of hot plasma	$\sim 3 \times 10^{53}$ ergs

* The distance to the galactic center is taken to be 8 kpc.

† 10-keV (1.2×10^8 K) thin hot plasma detected by Koyama *et al.* (1989).

(10 keV), we estimate the total mass of the plasma to be $\sim 2 \times 10^4 M_{\odot}$, and the thermal energy to be $\sim 3 \times 10^{53}$ ergs. The density is estimated approximately to be 8×10^{-2} H atoms cm⁻³.

Table 1 summarizes the derived parameters. These estimates indicate that the ionized gas, including the interior hot component, shares a small fraction of the total mass of the expanding ring. One can also see that the kinetic energy of the expanding motion of the ring is by an order of magnitude greater than the thermal energy involved in the hot interior. This is consistent if the hot interior is a remnant of shock-heated gas by an explosion near the center, similar to the case of shell-type supernova remnants: The energy released at the galactic center is mainly carried by the shock wave as the kinetic energy. The kinetic energy is partly used for heating up the gas, and the shock-heated gas remains at high temperature as the hot interior. However, the majority of the kinetic energy is carried with the expanding shell/cylinder and focuses on the 200-pc ring.

3. DISCUSSION

We have shown that the 200-pc (180-pc) expanding ring is a structure elongated in the direction perpendicular to the galactic plane and has a cylindrical shape. We have also shown that the cylinder is a mixture of molecular and ionized hydrogen gases. The existence of ionized gas is reasonable for the high expansion velocity of the ring, 110 km s⁻¹, which is extremely supersonic in the gaseous disk: The expanding cylinder at a supersonic velocity should certainly ionize the interstellar medium just behind the shock front, when it propagates through the disk and halo.

The radio continuum and CO spurs apparently overlap each other, and no

significant positional displacement in the longitude direction is seen. This positional coincidence suggests that the ionized, high-temperature gas and the molecular gas coexist within the cylinder wall. This may result if the ionized and molecular gases are in the form of filaments and/or clumps of smaller scales than the wall thickness (≤ 15 pc), which is in fact seen in the position-velocity diagram of the CO emission (Bally *et al.*, 1987, 1988).

A vertical outflow of a mixture of molecular and ionized gases ($H\alpha$ and dark filaments) has been observed in the starburst galaxy M82 associated with a molecular ring-and-cylinder structure of radius ~ 200 pc (Nakai *et al.*, 1987). The present result suggests that the Galactic 200-pc cylinder may be a similar object to the one found in M82. However, the energy is an order of magnitude less than that of M82 which is a few times 10^{55} ergs. This may simply be explained by the difference in the level of activity in the centers of the two galaxies. We may therefore suggest that the 200-pc molecular cylinder in our Galaxy may be a similar vertical outflow driven by a starburst and/or explosion near the center.

We also mention the similarity between the 6.7-keV iron-line feature showing the existence of very hot gas confined interior to the 200-pc cylinder (Koyama *et al.*, 1989) and the X-ray (0.1–4 keV) feature observed in M82 where the hot plasma is also channeled by the molecular cylinder and is more extended in the direction of the outflow, or perpendicular to the plane of the disk (Watson *et al.*, 1984; Nakai *et al.*, 1987). The X-ray luminosity of M82, 2×10^{40} ergs s^{-1} , is three orders of magnitude greater than the one at the galactic center; this may again simply be attributed to the different activity scales in the two galaxies. From this similarity it is predicted that the hard X-ray feature in the galactic center is extended in the direction perpendicular to the galactic plane, being channeled by the 200-pc cylinder. It would now be desirable to make a detailed map of this hot component and to make clear the spatial relationship to the molecular cylinder. In particular, the extent in the direction perpendicular to the galactic plane may give a clue to clarify if this is related to some outflow effect.

Formation of a cylindrical shock front in the galactic center has been studied numerically (Sakashita 1971; Sofue 1976, 1977, 1984; Saito and Saito 1977; Tomisaka and Ikeuchi 1987; Umemura *et al.*, 1987): In these models it is shown that an intense energy release at the center, such as due to an explosion and/or star bursts, causes a strong shock wave. The shock front, which was originally spherical, then becomes elongated in the direction perpendicular to the disk and attains a cylindrical shape. The Galactic Center Lobe (Sofue and Handa 1984) could be such a cylinder that is in the most-elongated phase of the shock front.

Due to refraction of the propagation path of the shock wave in the galactic disk and halo, a significant part of the cylinder wall (shock front) is then bent toward the disk, and focuses to a ring. According to the model, the radius of this “focal ring” is a few times the scale height of the gas disk (Sofue 1976), which is consistent with the observed radius of the expanding 200-pc ring. The models also show that a high-temperature gas remains uncooled in the region interior to the shock front because the cooling time scale is much longer than that of the shock for its low density and high temperature, and seems consistent with the existence of the X-ray emitting hot gas as mentioned above.

REFERENCES

- Bally, J., Stark, A. A., Wilson, R. W., and Henkel, C., 1987, *Astrophys. J. Suppl.*, **65**, 13.
- Bally, J., Stark, A. A., Wilson, R. W., and Henkel, C., 1988, *Astrophys. J.*, **324**, 223.
- Beichman, C. A., Neugebauer, G., Habing, H. J., Clegg, P. E., and Chester, T. J. (ed.) 1985, *IRAS Explanatory Supplement 1985*, JPL D-1855 (Jet Propulsion Laboratory, Pasadena).
- Fürst, E., Sofue, Y., and Reich, W., 1987, *Astron. Astrophys.*, **191**, 303.
- Handa, T., Sofue, Y., Nakai, N., Inoue, M., and Hirabayashi, H., 1987, *Pub. Astr. Soc. Japan*, **39**, 709.
- Kaifu, N., Iguchi, T., and Kato, T., 1974, *Publ. Astr. Soc. Japan*, **26**, 117.
- Kaifu, N., Kato, T., and Iguchi, T., 1972, *Nature*, **238**, 105.
- Koyama, K., Awaki, H., Kunieda, H., Takano, S., Tawara, S., Yamanuchi, S., Hatsukade, I., and Nagase, F., 1989, *Nature*, **339**, 603.
- Nakai, N., Hayashi, M., Handa, T., Sofue, Y., Hasegawa, T., and Sasaki, M., 1987, *Pub. Astr. Soc. Japan*, **39**, 685.
- Reich, W., Fürst, E., Steffen, P., Reif, K., and Haslam, C. G. T. 1984, *Astron. Astrophys. Suppl.*, **58**, 197.
- Reich, W., Sofue, Y., and Fürst, E., 1987, *Pub. Astr. Soc. Japan*, **39**, 573.
- Saito, M., and Saito, Y., 1977, *Pub. Astr. Soc. Japan*, **29**, 387.
- Sakashita, S., 1971, *Astrophys. Space Sci.*, **14**, 431.
- Scoville, N. Z., 1972, *Astrophys. J. Lett.*, **175**, L127.
- Sofue, Y., 1976, *Pub. Astr. Soc. Japan*, **28**, 19.
- Sofue, Y., 1977, *Astron. Astrophys.*, **60**, 327.
- Sofue, Y., 1984, *Pub. Astr. Soc. Japan*, **36**, 539.
- Sofue, Y., and Handa, T., 1984, *Nature*, **310**, 568.
- Sofue, Y., and Reich, W., 1979, *Astron. Astrophys. Suppl.*, **38**, 251.
- Solomon, P. M., Scoville, N. Z., and Sanders, D. B., 1979, *Astrophys. J. Letters*, **232**, L89.
- Tomisaka, K., and Ikeuchi, S., 1987, *Astrophys. J.*, **330**, 695.
- Umemura, S., Iki, K., Shibata, K., and Sofue, Y., 1988, *Pub. Astr. Soc. Japan*, **40**, 25.
- Watson, M. G., Stanger, V., and Griffiths, R. E., 1984, *Astrophys. J.*, bf 176, L144.